

SELF-SUPERVISED LEARNING FOR GASTRITIS DETECTION WITH GASTRIC X-RAY IMAGES

Guang Li[†] Ren Togo^{††} Takahiro Ogawa^{†††} Miki Haseyama^{†††}

[†] Graduate School of Information Science and Technology, Hokkaido University, Japan

^{††} Education and Research Center for Mathematical and Data Science, Hokkaido University, Japan

^{†††} Faculty of Information Science and Technology, Hokkaido University, Japan

E-mail: {guang, togo, ogawa}@lmd.ist.hokudai.ac.jp, miki@ist.hokudai.ac.jp

ABSTRACT

We propose a novel self-supervised learning method for medical image analysis. Great progress has been made in medical image analysis because of the development of supervised learning based on deep convolutional neural networks. However, annotating complex medical images usually requires expert knowledge, making it difficult for a wide range of real-world applications (*e.g.*, computer-aided diagnosis systems). Our self-supervised learning method introduces a cross-view loss and a cross-model loss to solve the insufficient available annotations in medical image analysis. Experimental results show that our method can achieve high detection performance for gastritis detection with only a small number of annotations.

Index Terms— Self-supervised learning, gastritis detection, gastric X-Ray image.

1. INTRODUCTION

With the development of supervised learning based on Deep Convolutional Neural Networks (DCNNs), great progress has been made in medical image analysis, such as disease detection and organ segmentation [1, 2]. Supervised learning approaches generally benefit from a large number of well-annotated training samples [3]. Crowdsourcing and semi-automatic software tools are utilized since the annotation of natural images requires only simple human knowledge [4]. However, generating annotations of complex medical images usually requires expert knowledge and hence is expensive and time-consuming [5, 6]. Consequently, the scarcity of expert-level annotations is one of the main obstacles for real-world applications in medical image analysis [7].

Self-supervised learning has recently attracted widespread attention in machine learning as a development form of supervised learning [8]. Unlike supervised learning using manually annotated labels, self-supervised learning aims to learn from the image characteristics (*e.g.*, texture, position and color) without label information [9]. Many self-supervised learning methods have been proposed to learn discriminative representations based on pretext tasks. For example, [10] predicts rotation degrees of the images, and [11] learns semantic information by playing a jigsaw game on the images. Subsequently, we can use the model trained with self-supervised learn-

ing to perform fine-tuning on the target downstream tasks. Since the fine-tuning process requires only a small portion of annotated data, it provides a feasible solution for insufficient data annotations.

Among the self-supervised learning methods, contrastive-based self-supervised learning methods have shown to be effective for natural images [12]. Contrastive learning methods aim at reducing the distance between representations of different views augmented from the same images (*i.e.*, positive sample pairs) and increasing the distance between representations of views augmented from different images (*i.e.*, negative sample pairs). Since the negative sample pairs can help spread out the features on the hypersphere, they can improve the representation learning performance and prevent the learning from collapsing. Some methods utilize different tricks to increase the number of negative sample pairs for improving the representation learning performance. For example, [13] uses large batch size directly, [14] uses a memory bank, and [15] incorporates online clustering in the training process. However, requiring large number of negative sample pairs is inefficient for the learning of discriminative representations, especially for high-resolution medical images [16].

Recently, the contrastive-based self-supervised learning method BYOL [17] has achieved state-of-the-art performance on the large-scale natural image dataset ImageNet [18] without negative sample pairs. Not requiring a negative sample is efficient to process medical images with high resolution and more complex semantic information. Specifically, BYOL conducts contrastive learning by reducing the distance between representations of two different views from the teacher-student networks directly. The teacher-student architecture is considered useful for self-supervised learning, and we introduce a more explicit contrastive learning method to learn discriminative representations.

In this paper, we propose a novel self-supervised learning method for medical image analysis. Different from BYOL, we newly introduce a cross-view loss and a cross-model loss to the self-supervised learning, which can conduct more explicit contrastive learning and learn more semantic information from medical images. Specifically, we perform the contrastive learning by reducing the distance between representations of two different views from the student network and reducing the distance between representations of the same view from the teacher-student networks. Experimental results showed that our method can achieve high detection performance for the gastritis detection task with only a small number of annotations.

Our contributions are summarized as follows.

- We propose a novel self-supervised learning method for medical image analysis, which introduces a cross-view loss and a

The experimental data were provided by The University of Tokyo Hospital in Japan. We express our thanks to Katsuhiko Mabe of the Junpukai Health Maintenance Center and Nobutake Yamamichi of the Graduate School of Medicine, The University of Tokyo. This research was supported in part by the JSPS KAKENHI under Grant JP17H01744 and Grant JP20K19857, and in part by the Photo-Excitonix Project of Hokkaido University.

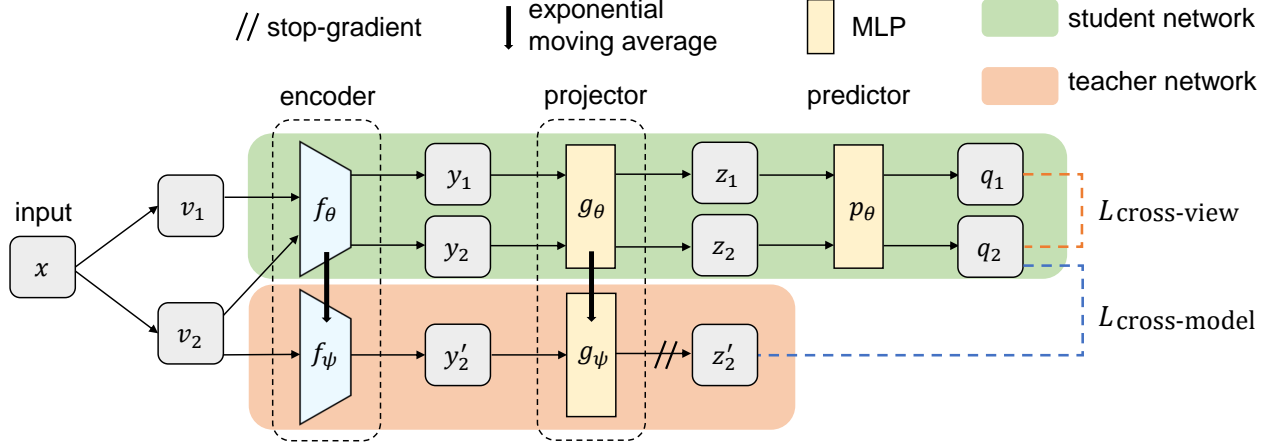


Fig. 1. Overview of the proposed method. Our method minimizes (1) a cross-view loss between representations of two views from the student network and (2) a cross-model loss between representations of the same view from the teacher-student networks. The weights of the teacher network (ψ) are an exponential moving average of the weights of the student network (θ). MLP denotes multilayer perceptron.

cross-model loss.

- We realize high detection performance in a complex gastric X-Ray image dataset with only a small number of annotations.

2. SELF-SUPERVISED LEARNING FOR GASTRITIS DETECTION

This section shows the details of the proposed method. Figure 1 shows an overview of our method. In subsection 2.1, we show the preprocessing of the gastric X-Ray images. Then we demonstrate the self-supervised learning in subsection 2.2. Finally, we show how to perform fine-tuning and gastritis detection in subsection 2.3.

2.1. Gastric Image Data Preprocessing

The resolution of the patient-level gastric X-Ray images in our dataset is $2,048 \times 2,048$ pixels. In addition, there is only a small number of images in the dataset. To make full use of the semantic information of the gastric X-Ray images, we divide each patient-level image into patches and manually annotate them with the following three labels:

- \mathcal{O} : patches outside the stomach (outside patches),
- \mathcal{N} : patches extracted from negative (non-gastritis) X-Ray images inside the stomach (negative patches),
- \mathcal{P} : patches extracted from positive (gastritis) X-Ray images inside the stomach (positive patches).

Figure 2 shows the examples of patient-level gastric X-Ray images. We can see that the stomach without gastritis (Fig. 2 (a)) has straight folds and uniform mucosal surface patterns. On the other hand, the stomach with gastritis (Fig. 2 (b)) has non-straight folds and coarse mucosal surface patterns.

2.2. Proposed Self-supervised Learning

Our method utilizes a teacher-student architecture (f_θ , p_θ and g_θ belonging to the student network, and f_ψ and g_ψ belonging to the teacher network) to learn discriminative representations from the

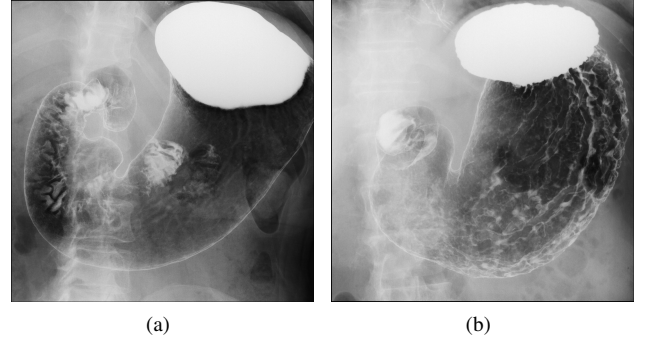


Fig. 2. Examples of patient-level gastric X-Ray images: (a) negative image, (b) positive image.

gastric patches. First, we obtain two randomly augmented views v_1 and v_2 from an input patch x . The view v_1 is processed by the encoder network f_θ and the projector g_θ of the student network. Accordingly, the view v_2 is processed by the encoder network f_ψ and the projector g_ψ of the teacher network (z'_2 is the final output of v_2). Specifically, we make a copy of v_2 and input it into the student network for the final loss calculation. Next, we use the predictor p_θ to transform the final outputs of two views as q_1 and q_2 in the student network. Note that g_θ , g_ψ and p_θ are MLP layers with the same architecture [13]. Finally, we define the cross-view loss and the cross-model loss between the normalized predictions and projections.

Cross-view loss. The cross-view loss defined by the following equation compares representations of two views from the student network, which penalizes different predictions for the views from positive pairs:

$$\begin{aligned} \mathcal{L}_{\text{cross-view}} &= \|\hat{q}_1 - \hat{q}_2\|_2^2 \\ &= 2 - 2 \cdot \frac{\langle q_1, q_2 \rangle}{\|q_1\|_2 \cdot \|q_2\|_2}, \end{aligned} \quad (1)$$

where $\hat{q}_1 = q_1/\|q_1\|_2$ and $\hat{q}_2 = q_2/\|q_2\|_2$ denote the normalized predictions of v_1 and v_2 from the student network, respectively.

Cross-model loss. The cross-model loss defined by the following equation compares representations of the same view from the teacher-student networks, which penalizes different prediction and projection for the same view from different networks:

$$\begin{aligned}\mathcal{L}_{\text{cross-model}} &= \|\hat{q}_2 - \hat{z}'_2\|_2^2 \\ &= 2 - 2 \cdot \frac{\langle q_2, z'_2 \rangle}{\|q_2\|_2 \cdot \|z'_2\|_2},\end{aligned}\quad (2)$$

where $\hat{z}'_2 = z'_2/\|z'_2\|_2$ denotes the normalized projection of v_2 from the teacher network. Note that we only apply the predictor in the student network to make the teacher-student architecture asymmetric, which can have a better representations learning performance [17]. Since the consistency between the predictions from the teacher-student networks have been proved effective in semi-supervised learning [19], we introduce the cross-model loss into our self-supervised learning method. We update the weights of the student network (θ) by minimizing a total loss that combines the cross-view loss and the cross-model loss. The total loss $\mathcal{L}_{\theta,\psi}$ and optimizing process are defines as follows:

$$\mathcal{L}_{\theta,\psi} = \beta \mathcal{L}_{\text{cross-view}} + (1 - \beta) \mathcal{L}_{\text{cross-model}}, \quad (3)$$

$$\theta \leftarrow \text{Opt}(\theta, \nabla_{\theta} \mathcal{L}_{\theta,\psi}, \alpha), \quad (4)$$

where β ($0 \leq \beta \leq 1$) is an balance-weight between the cross-view loss and the cross-model loss. In addition, Opt and α denote an optimizer and the learning rate, respectively. The weights of the teacher network (ψ) are an exponential moving average of the weights of the student network (θ) and are updated as follows:

$$\psi \leftarrow \tau \psi + (1 - \tau) \theta, \quad (5)$$

where τ denotes the degree of moving average, and we update the weights after every iteration. Since the stop-gradient operation plays an essential role to prevent the learning from collapsing [20], we keep the teacher network not updated by backpropagation. With the self-supervised learning, the student network can learn sufficient semantic information from the patches and can be used for fine-tuning and gastritis detection.

2.3. Fine-tuning and Gastritis Detection

After the self-supervised learning, we fine-tune the encoder of the student network (f_{θ}) with only a small number of annotated images. In the test phase, we also divide the patient-level gastric X-Ray images into patches as shown in subsection 2.1. Then we load the divided patches into the fine-tuned DCNN model and predict the labels of these patches. Subsequently, we calculate the number of patches \mathcal{N} and \mathcal{P} , respectively. We do not count the number of patches \mathcal{O} because these patches outside the stomach are not related to the final gastritis detection. Finally, we predict the label of a patient-level gastric X-Ray image as follows:

$$y^{\text{test}} = \begin{cases} 1 & \text{if } \frac{\sum(\mathcal{P})}{\sum(\mathcal{N}) + \sum(\mathcal{P})} \geq \sigma, \\ 0 & \text{otherwise} \end{cases}, \quad (6)$$

where $\sum(\mathcal{N})$ and $\sum(\mathcal{P})$ denote the numbers of negative patches and positive patches, respectively. σ is a threshold that can be adjusted according to different experimental conditions. If $y^{\text{test}} = 1$, the predict label of a patient-level gastric X-Ray image is positive, and the predict label is negative if $y^{\text{test}} = 0$.

3. EXPERIMENTS

In this section, we conduct the experiments to verify the effectiveness of the proposed method. In subsection 3.1, we show the dataset in the experiments. Then we demonstrate the experimental settings and results in subsections 3.2 and 3.3, respectively. All of our experiments were conducted by using PyTorch [21] framework with an NVIDIA Tesla P100 GPU.

3.1. Dataset

The dataset used in our research contains 815 patients' (240 positive and 575 negative) gastric X-Ray images. Each image had a ground truth label (positive/negative), which was determined by the diagnostic results of X-Ray inspection and endoscopic examination. We used 200 patients' images (100 positive and 100 negative) as a training data and the rest as a test data. As shown in the subsection 2.1, we first divided the gastric X-Ray images into patches. The patch size and the sliding interval were set to 299 pixels and 50 pixels as the same as our previous researches [22, 23]. The patches in the training data were annotated as \mathcal{O} , \mathcal{N} and \mathcal{P} by a radiological technologist. Note that if the area inside the stomach in the patch was less than 1%, the patch was annotated as \mathcal{O} . In addition, if the area inside the stomach in the patch was more than 85%, the patch was annotated as \mathcal{N} or \mathcal{P} . We discarded the rest of the patches in the training data. The numbers of obtained \mathcal{O} , \mathcal{N} and \mathcal{P} patches were 48,385, 42,785 and 45,127, respectively.

We took the obtained 200 patients' patches as our training data for the self-supervised learning process and did not use their label information. Moreover, we split the 200 patients' patches into the data of 120 and 80 patients' patches (half positive and half negative) as training data and validation set of the fine-tuning process. Then we randomly selected 10, 20, 30 and 40 patients' patches (half positive and half negative) from the 120 patients' training data as training sets of the fine-tuning process, respectively.

3.2. Implementation

In the self-supervised learning process, we generated views with a view generator that combined with the cropping, resizing, flipping, color jitter and Gaussian blur as the same as [24]. The generated view size was set to 128 experimentally. We used the ResNet50 [25] network as our encoders f_{θ} and f_{ψ} , whose output feature dimension was 2,048 (the output of the final average pooling layer). The projectors g_{θ} and g_{ψ} and the predictor p_{θ} had the same architecture, which consisted of a linear layer with output size 4,096, a batch normalization layer, a ReLU activation function and a linear layer with output size 256. The optimizer used in our method was an SGD optimizer, whose learning rate α , momentum and weight decay were set to 0.03, 0.9, 0.0004, respectively. Moreover, we performed 80 epochs in the self-supervised learning process.

In the fine-tuning process, we used the weights of the trained encoder in the student network (f_{θ}) as the initial weights. We assume that the effect of self-supervised learning is positively correlated with the final gastritis detection performance. To verify the effectiveness of the proposed method (PM), we used the following methods as comparative methods.

CM1. We used the weights of the trained encoder of the state-of-the-art method BYOL [17] as the initial weights for the fine-tuning process.

CM2. We used the weights of the trained encoder of the state-of-the-art method PIRL [26] based on the jigsaw pretext task as the

Table 1. Gastritis detection results after fine-tuning on the data of 10, 20, 30 and 40 patients in Ex. I.

Method	10 patients			20 patients			30 patients			40 patients		
	Sen	Spe	HM	Sen	Spe	HM	Sen	Spe	HM	Sen	Spe	HM
PM	0.957	0.806	0.875	0.964	0.863	0.911	0.936	0.895	0.915	0.964	0.901	0.931
CM1	0.964	0.758	0.849	0.907	0.920	0.913	0.807	0.956	0.875	0.964	0.861	0.910
CM2	0.721	0.806	0.761	0.943	0.507	0.659	0.879	0.743	0.805	0.864	0.737	0.795
CM3	0.607	0.735	0.665	0.929	0.316	0.472	0.879	0.440	0.586	0.886	0.632	0.738
CM4	0.236	1.000	0.382	0.850	0.686	0.759	0.279	0.989	0.435	0.864	0.876	0.870
CM5	0.771	0.225	0.348	0.693	0.364	0.477	0.457	0.734	0.563	0.579	0.726	0.644

initial weights for the fine-tuning process.

CM3. We used the weights of the trained encoder of PIRL [26] based on the rotation prediction pretext task as the initial weights for the fine-tuning process.

CM4. We used the weights of the pre-trained model of ImageNet as the initial weights for the fine-tuning process.

CM5. We used random weights as the initial weights for the fine-tuning process.

We conducted two experiments for verification of the effectiveness of the proposed method and analysis of the hyperparameter. In the experiment I (Ex. I), we conducted self-supervised learning with the condition of loss weight $\beta = 0.5$ and fine-tuned the trained encoder on all of the four training sets. In the experiment II (Ex. II), we conducted self-supervised learning with the condition of different loss weights and fine-tuned the trained encoder on all of the four training sets. In both of the experiments, we selected the model that has the highest accuracy on the validation set and tested the gastritis detection performance on the test set of 615 patients' data. Note that the settings of the BYOL method used in our experiments were the same as the proposed method. The settings of the PIRL method used in our experiments were under the guidance of [26] except for the batch size and the number of negative sample pairs due to the limitations of our computing resources. Moreover, we used the same settings in the fine-tuning process in both of the experiments.

In the test phase, we set the threshold σ to 0.5 experimentally. We utilized the following sensitivity (Sen), specificity (Spe) and harmonic mean (HM) of the sensitivity and specificity as evaluation metrics:

$$\text{Sen} = \frac{\text{TP}}{\text{TP} + \text{FN}}, \quad (7)$$

$$\text{Spe} = \frac{\text{TN}}{\text{TN} + \text{FP}}, \quad (8)$$

$$\text{HM} = \frac{2 \times \text{Sen} \times \text{Spe}}{\text{Sen} + \text{Spe}}, \quad (9)$$

where TP, TN, FP and FN denote the number of true positive, true negative, false positive and false negative, respectively. Since Sen and Spe have a trade-off relationship, we took the HM as the final evaluation metric.

3.3. Results and Discussion

The experimental results are shown in Table 1. Table 1 shows the patient-level gastritis detection results after fine-tuning on the data of 10, 20, 30 and 40 patients in Ex. I. From Table 1, we can see that the proposed method that introduces the cross-view loss and the cross-model loss achieves the highest gastritis detection performance compared with other comparative methods. The most used pre-trained model of ImageNet has an HM score of 0.870 with 40 patients' annotations. However, our method achieves an HM score

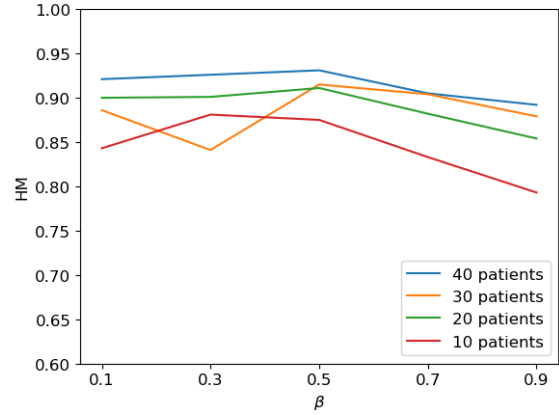


Fig. 3. Gastritis detection results of PM with different loss weights after fine-tuning on the data of 10, 20, 30 and 40 patients in Ex. II.

of 0.875 with only 10 patients' annotations. Experimental results have shown that our method realizes high gastritis detection performance with only a small number of annotations.

Figure 3 shows the gastritis detection results with different loss weights after fine-tuning on the data of 10, 20, 30 and 40 patients in Ex. II. From Fig. 3, we can see that when β approaches 0.5, the gastritis detection performance tends to have a higher HM score, indicating that the balance of the cross-view loss and the cross-model loss was useful for learning discriminative representations.

We compared the proposed method with the two state-of-the-art self-supervised learning methods in our experiments. Many other self-supervised learning methods were emerging recently, such as SimCLR [13] and MoCo [14], which used multiple TPUs or GPUs. Due to the limitations of our computing resources, we did not conduct comparative experiments with these methods. However, the experimental results showed that the proposed method can learn discriminative representations with only a single GPU on the complex gastric X-Ray image dataset.

4. CONCLUSION

We have proposed a novel self-supervised learning method for medical image analysis. We introduce the cross-view loss and the cross-model loss to the self-supervised learning, which can conduct more explicit contrastive learning and learn more semantic information from medical images. Experimental results have shown that our method can achieve high patient-level detection performance for gastritis detection with only a small number of annotations.

5. REFERENCES

- [1] Alex Krizhevsky, Ilya Sutskever, and Geoffrey E Hinton, “Imagenet classification with deep convolutional neural networks,” *Communications of the ACM*, vol. 60, no. 6, pp. 84–90, 2017.
- [2] Dinggang Shen, Guorong Wu, and Heung-Il Suk, “Deep learning in medical image analysis,” *Annual review of biomedical engineering*, vol. 19, pp. 221–248, 2017.
- [3] Alex Krizhevsky, Ilya Sutskever, and Geoffrey E Hinton, “Imagenet classification with deep convolutional neural networks,” in *Proceedings of the Advances in Neural Information Processing Systems (NeurIPS)*, 2012, pp. 1097–1105.
- [4] Olga Russakovsky, Jia Deng, Hao Su, Jonathan Krause, Sanjeev Satheesh, Sean Ma, Zhiheng Huang, Andrej Karpathy, Aditya Khosla, Michael Bernstein, et al., “Imagenet large scale visual recognition challenge,” *International Journal of Computer Vision*, vol. 115, no. 3, pp. 211–252, 2015.
- [5] Liang Chen, Paul Bentley, Kensaku Mori, Kazunari Misawa, Michitaka Fujiwara, and Daniel Rueckert, “Self-supervised learning for medical image analysis using image context restoration,” *Medical Image Analysis*, vol. 58, pp. 101539, 2019.
- [6] Zongwei Zhou, Vatsal Sodha, Md Mahfuzur Rahman Siddiquee, Ruibin Feng, Nima Tajbakhsh, Michael B Gotway, and Jianming Liang, “Models genesis: Generic autodidactic models for 3d medical image analysis,” in *International Conference on Medical Image Computing and Computer-Assisted Intervention (MICCAI)*, 2019, pp. 384–393.
- [7] Aiham Taleb, Christoph Lippert, Tassilo Klein, and Moin Nabi, “Multimodal self-supervised learning for medical image analysis,” *arXiv preprint arXiv:1912.05396*, 2019.
- [8] Xiao Liu, Fanjin Zhang, Zhenyu Hou, Zhaoyu Wang, Li Mian, Jing Zhang, and Jie Tang, “Self-supervised learning: Generative or contrastive,” *arXiv preprint arXiv:2006.08218*, 2020.
- [9] Longlong Jing and Yingli Tian, “Self-supervised visual feature learning with deep neural networks: A survey,” *IEEE Transactions on Pattern Analysis and Machine Intelligence*, 2020.
- [10] Spyros Gidaris, Praveer Singh, and Nikos Komodakis, “Unsupervised representation learning by predicting image rotations,” in *Proceedings of the International Conference on Learning Representations (ICLR)*, 2018.
- [11] Mehdi Noroozi and Paolo Favaro, “Unsupervised learning of visual representations by solving jigsaw puzzles,” in *Proceedings of the European Conference on Computer Vision (ECCV)*, 2016, pp. 69–84.
- [12] Ashish Jaiswal, Ashwin Ramesh Babu, Mohammad Zaki Zadeh, Debapriya Banerjee, and Fillia Makedon, “A survey on contrastive self-supervised learning,” *arXiv preprint arXiv:2011.00362*, 2020.
- [13] Ting Chen, Simon Kornblith, Mohammad Norouzi, and Geoffrey Hinton, “A simple framework for contrastive learning of visual representations,” in *Proceedings of the International Conference on Machine Learning (ICML)*, 2020.
- [14] Kaiming He, Haoqi Fan, Yuxin Wu, Saining Xie, and Ross Girshick, “Momentum contrast for unsupervised visual representation learning,” in *Proceedings of the IEEE/CVF Conference on Computer Vision and Pattern Recognition (CVPR)*, 2020, pp. 9729–9738.
- [15] Mathilde Caron, Ishan Misra, Julien Mairal, Priya Goyal, Piotr Bojanowski, and Armand Joulin, “Unsupervised learning of visual features by contrasting cluster assignments,” in *Proceedings of the Advances in Neural Information Processing Systems (NeurIPS)*, 2020.
- [16] Yuandong Tian, Lantao Yu, Xinlei Chen, and Surya Ganguli, “Understanding self-supervised learning with dual deep networks,” *arXiv preprint arXiv:2010.00578*, 2020.
- [17] Jean-Bastien Grill, Florian Strub, Florent Altché, Corentin Tallec, Pierre Richemond, Elena Buchatskaya, Carl Doersch, Bernardo Avila Pires, Zhaohan Guo, Mohammad Gheshlaghi Azar, et al., “Bootstrap your own latent—a new approach to self-supervised learning,” in *Proceedings of the Advances in Neural Information Processing Systems (NeurIPS)*, 2020.
- [18] Jia Deng, Wei Dong, Richard Socher, Li-Jia Li, Kai Li, and Li Fei-Fei, “Imagenet: A large-scale hierarchical image database,” in *Proceedings of the IEEE Conference on Computer Vision and Pattern Recognition (CVPR)*, 2009, pp. 248–255.
- [19] Antti Tarvainen and Harri Valpola, “Mean teachers are better role models: Weight-averaged consistency targets improve semi-supervised deep learning results,” in *Proceedings of the Advances in Neural Information Processing Systems (NeurIPS)*, 2017, pp. 1195–1204.
- [20] Xinlei Chen and Kaiming He, “Exploring simple siamese representation learning,” *arXiv preprint arXiv:2011.10566*, 2020.
- [21] Adam Paszke, Sam Gross, Francisco Massa, Adam Lerer, James Bradbury, Gregory Chanan, Trevor Killeen, Zeming Lin, Natalia Gimelshein, Luca Antiga, et al., “Pytorch: An imperative style, high-performance deep learning library,” in *Proceedings of the Advances in Neural Information Processing Systems (NeurIPS)*, 2019, pp. 8024–8035.
- [22] Guang Li, Ren Togo, Takahiro Ogawa, and Miki Haseyama, “Soft-label anonymous gastric x-ray image distillation,” in *Proceedings of the IEEE International Conference on Image Processing (ICIP)*, 2020, pp. 305–309.
- [23] Ren Togo, Takahiro Ogawa, and Miki Haseyama, “Multimodal image-to-image translation for generation of gastritis images,” in *Proceedings of the IEEE International Conference on Image Processing (ICIP)*, 2020, pp. 2466–2470.
- [24] Yonglong Tian, Chen Sun, Ben Poole, Dilip Krishnan, Cordelia Schmid, and Phillip Isola, “What makes for good views for contrastive learning,” in *Proceedings of the Advances in Neural Information Processing Systems (NeurIPS)*, 2020.
- [25] Kaiming He, Xiangyu Zhang, Shaoqing Ren, and Jian Sun, “Deep residual learning for image recognition,” in *Proceedings of the IEEE/CVF Conference on Computer Vision and Pattern Recognition (CVPR)*, 2016, pp. 770–778.
- [26] Ishan Misra and Laurens van der Maaten, “Self-supervised learning of pretext-invariant representations,” in *Proceedings of the IEEE/CVF Conference on Computer Vision and Pattern Recognition (CVPR)*, 2020, pp. 6707–6717.